Polymer 50 (2009) 6228–6234

Contents lists available at ScienceDirect

Polymer

journal homepage: www.elsevier.com/locate/polymer

Miscible blends of poly(butyl methacrylate) densely grafted on fumed silica with poly(vinyl chloride)

Kenichi Hayashida*, Hiromitsu Tanaka, Osamu Watanabe

Organic Materials Research Lab, Toyota Central R&D Labs., Inc., Nagakute, Aichi 480-1192, Japan

ARTICLE INFO

Article history:
Received 10 September 2009
Received in revised form
29 October 2009
Accepted 4 November 2009
Available online 10 November 2009

Keywords:
Surface-initiated atom transfer radical polymerization
Nanocomposite
Miscible blend

ABSTRACT

Poly(butyl methacrylate) (PBMA) densely grafted on a fumed silica particle consisting of primary particles with an average diameter of 14 nm, has been synthesized by surface-initiated atom transfer radical polymerization (SI-ATRP). In these syntheses, a newly designed initiator, *p*-(bromomethyl)benzyl 2-bromoisobutylate was used for the immobilization of the initiator moiety on the silica particle to give the densely grafted PBMA. Thus synthesized nanocomposites have exhibited unusual miscibility with poly(vinyl chloride) (PVC) through differential scanning calorimetry (DSC). The derivative DSC peaks for the composite/PVC blends were significantly different from those for the conventional PBMA/PVC blends. This interesting finding is due to a wide gradient of the PVC concentration on a microscopic scale, resulting from the densely grafted PBMA chains; the PBMA component is enriched near the surface of the fumed silica, while the PVC component is enriched far from the surface. This gradient miscible state is strongly supported by dynamic mechanical analysis. Furthermore, a synergistic effect on storage modulus was seen in the nanocomposite/PVC blends.

1. Introduction

Polymer/inorganic nanocomposite materials have remarkably been developed for the last few decades [1–9]. Generally, in these materials, nano-sized inorganic fillers are dispersed in polymer matrices. The inorganic fillers include silica particles, layered silicates (e.g., montmorillonaite, mica), carbon materials (e.g., carbon black, carbon nanotube), nanoparticles of metals and metal oxides (e.g., Au, Ag, TiO_2, Fe_3O_4), and so on. Among these inorganic fillers, silica particles, such as fumed and colloidal silica, are one of the most widely used materials because of their advantages of stiffness, dielectricity, chemical stability, availability and inexpensiveness; especially, fumed silica is effective in reinforcement of polymeric materials due to its large specific surface area and relatively high aspect ratio. Polymer/silica nanocomposites, therefore, have attracted not only academic interest but also industrial one [10,11].

On the other hand, interfaces between the polymers and the inorganic fillers play a dominant role in properties of the nanocomposites. Strong interaction at the interface often leads to good mechanical properties; stiffness, tensile and impact strengths. Therefore, the surfaces of inorganic fillers have commonly been treated with organic agents, such as silane coupling agents. Polymer grafting is also promising for modification of the fillers [12–27]. The technique of grafting polymer is divided into two methods, "grafting-to" and "grafting from". The "grafting-to" method involves the reaction of reactive macromolecules and functional groups on fillers [12–14]. Though synthetically simple, "grafting-to" method has a number of disadvantages; most notably low graft density due to steric hindrance by the polymer chains. The "grafting from" method overcomes this serious limitation, where the surfaces of inorganic fillers are modified with initiators, and then monomers are polymerized [15–27]. "Grafting from" provide high graft densities because unlike polymer chains, the small monomers can easily approach the active sites for polymerization. The "Grafting from" method also referred to as surface-initiated polymerization (SIP). In recent years, SIP involving living polymerization (especially, living radical polymerization; e.g., atom transfer radical polymerization (ATRP) [28,29], reversible addition-fragmentation chain transfer polymerization [30]), or surface-initiated living polymerization (SILP) has been established to give controlled and/or concentrated polymer brushes [18–27]. The graft densities of the concentrated polymer brushes reach as high as 0.7 chains/nm^2 for common polymers, such as poly(methyl methacrylate) (PMMA) and polystyrene. Fukuda and coworkers have demonstrated that the glass transition temperature [31], compression resistance [32], and miscibility with free macromolecules [33], of the concentrated polymer brushes are quite different from those of semi-dilute brushes (less than 0.05 chains/nm^2) for the polymer brushes on inorganic substrates.

* Corresponding author. Tel.: +81 561 71 7247; fax: +81 561 63 6498.
E-mail address: e1440@mosk.tytlabs.co.jp (K. Hayashida).

0032-3861/$ – see front matter © 2009 Elsevier Ltd. All rights reserved.
doi:10.1016/j.polymer.2009.11.008

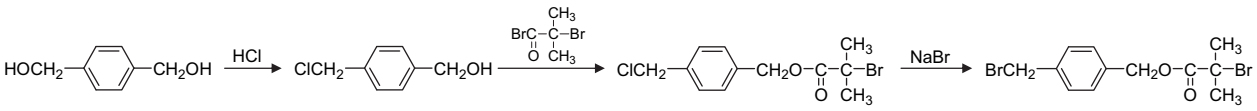

Scheme 1.

Also, a new family of colloidal crystals was identified for a nanocomposite consisting of PMMA densely grafted on spherical silica in solution [34]. However, no notable property in bulk has been reported for nanocomposites containing densely polymer-grafted nanoparticle; e.g., the densely grafted polymer itself and that dispersed in polymer matrix.

The concentrated polymer brush has already lost extensive chain conformational entropy due to the chain stretching perpendicular to the surface. Consequently, it occurs that the polymer brush excludes even the same kind of free polymer chains in condensed state, because the mixing causes further entropic loss for the graft chain conformation [33]. This phenomenon would be unfavorable for the mechanical strength of nanocomposites containing the densely grafted polymer, because of reduction in the entanglement between the polymer brushes or between the polymer brush and the matrix polymer. On the other hand, a question is raised as to what happens if a different polymer which is originally miscible with the graft polymer, is blended into the polymer brush. The densely grafted polymer might merge into the miscible different polymer due to the interaction between the two kinds of polymers. Furthermore, in the case of polymer chains densely grafted on a nano-particle, the number of the polymer chains per unit area is decreased as the chains are far from the curved surface of the particle. Therefore, in the mixture of a polymer densely grafted on the nano-particle and a miscible polymer, the miscible polymer chains are expected to be gradually enriched with increasing in the distance from the surface of the nano-particle. This type of blend of the nanocomposite with the miscible matrix polymer, must be different from both the original composite and a conventional miscible blend of the two kinds of polymers in many properties. Herein, we have demonstrated this strategy by a nanocomposite/miscible polymer blend system. In order to realize this concept, the nanocomposites consisting of poly(butyl methacrylate) (PBMA) densely grafted on a fumed silica nano-particle were synthesized by SILP technique using a newly designed initiator of ATRP, *p*-(bromomethyl)benzyl 2-bromoisobutylate. Thus synthesized nanocomposites were blended with poly(vinyl chloride) (PVC), which is miscible with PBMA [35–37]. The resultant nanocomposite/PVC blends were characterized by differential scanning calorimetry and dynamic mechanical analysis.

2. Experimental section

2.1. Synthesis of p-(bromomethyl)benzyl 2-bromoisobutylate (BBnBiB)

Monochlorination of *p*-xylene-α,α′-diol [38]: 300 ml of concentrated hydrochloric acid was added to 83 g (0.60 mol) of *p*-xylene-α,α′-diol dispersed in 1.2 L of toluene. After stirring for 9 h at room temperature, the oil layer was separated from the resultant mixture and washed with aqueous sodium sulfate. The solvent was removed by evaporation, and then the residual *p*-(chloromethyl)benzyl alcohol was recrystallized from chloroform.

Esterification of *p*-(chloromethyl)benzyl alcohol: A mixture of 100 g (0.44 mol) of bromoisobutyryl bromide and 100 ml of diethyl ether was added dropwise to a solution of 68 g (0.44 mol) of the purified *p*-(chloromethyl)benzyl alcohol in 300 ml of diethyl ether in the presence of 36 g (0.45 mol) of pyridine over 1 h at 0 °C. After stirring for an additional 2 h at room temperature, 300 ml of water was added. The oil layer was separated and washed with aqueous sodium hydrogen carbonate and aqueous sodium sulfate successively. Evaporation of the solution which had been dried over anhydrous sodium sulfate gave a residue of crude *p*-(chloromethyl)benzyl 2-bromoisobutylate.

Halogen exchange of *p*-(chloromethyl)benzyl 2-bromoisobutylate: 130 g (0.43 mol) of the crude *p*-(chloromethyl)benzyl 2-bromoisobutylate and 89 g (0.86 mol) of sodium bromide were heated at 60 °C for 1 h in 300 ml of *N*,*N*-dimethylformamide. Then, the mixture was cooled and filtered, and 10 g (0.1 mol) of sodium bromide added again. After heating for an additional 1 h, the product was extracted by a mixture of chloroform/water. Separation of the oil layer followed by evaporation gave a viscous residue of crude *p*-(bromomethyl)benzyl 2-bromoisobutylate (BBnBiB). The product was recrystallized from methanol repeatedly. ^{1}H NMR (400 MHz, $CDCl_3$): δ 1.95 (s, 6H), 4.50 (s, 2H), 5.20 (s, 2H), 7.3–7.4 (m, 4H). mp: 39–40 °C.

2.2. Synthesis of benzyl 2-bromoisobutylate (BnBiB)

A mixture of 23 g (0.10 mol) of 2-bromoisobutyryl bromide and 50 ml of diethyl ether was added dropwise to a solution of 13 g (0.12 mol) of benzyl alcohol in 100 ml of diethyl ether in the presence of 12 g (0.12 mol) of triethylamine over 0.5 h at 0 °C. After stirring for an additional 2 h at room temperature, 100 ml of water was added. The oil layer was separated and washed with aqueous sodium sulfate. Evaporation of the solution gave a residue of crude benzyl 2-bromoisobutylate (BnBiB). The liquid was purified by distillation under reduced pressure.

2.3. Synthesis of ATRP initiator-modified fumed silica

Amine-modification of fumed silica: 3.6 ml of *N*-[3-(trimethoxysilyl)propyl]aniline (15 mmol) and 0.8 ml of hexylamine (6 mmol) were added to 15 g of fumed silica with a primary particle diameter of 14 nm (Silica, fumed, $d = 2.2$ g/cm^3, Sigma) homogeneously dispersed in 380 ml of acetonitrile (AN). The dispersion was sonicated and kept at 50 °C for 6 h. The amine-modified silica was purified by 3

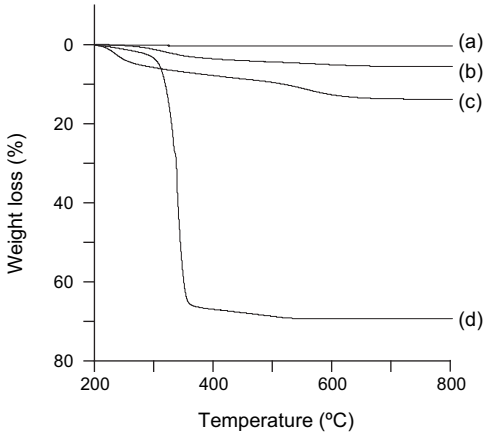

Fig. 1. TG curves of the modified fumed silica samples in an air flow. (a) Silica. (b) Silica-NHPh. (c) Silica-Br. (d) Silica-PBMA.

Table 1
Characteristics of the modified fumed silica particles.

Sample	$M_n \times 10^{-3}$[a]	M_w/M_n[a]	Loading[b] (μmol/g)
Silica-Br	–	–	370
Silica-PBMA	41	1.10	50

[a] Values for the free polymer formed from the unfixed initiator.
[b] Determined by TG in an air flow.

cycles of centrifugation and redispersion in AN. The purified amine-modified silica was dried and thermally treated at 130 °C for 2 h under vacuum.

Immobilization of ATRP initiator on fumed silica: 5.3 g of BBnBiB (15 mmol) and 1.9 g of proton-sponge (9.0 mmol) were added to 14.5 g of the amine-modified fumed silica homogeneously dispersed in 200 ml of AN. The mixture was sonicated and kept at 50 °C for 6 h. After dilution with 200 ml of *N*,*N*-dimethylacetamide (DMAc) followed by passing through a 5.0 μm PTFE membrane filter, the initiator-modified fumed silica was precipitated into methanol and purified by 3 cycles of centrifugation and redispersion in DMAc.

2.4. Surface-initiated polymerization using initiator-modified fumed silica in the presence of an unfixed initiator

A solution of 5.4 μl of BnBiB (30 μmol) in 30 ml of DMAc was added to 0.50 g of the initiator-modified fumed silica and 14.3 mg of CuBr (100 μmol) in a vacuum. After sonication of the mixture, 31.2 mg of bpy (200 μmol) in 30 ml of BMA was added, and the dispersion was kept at 60 °C for 1 h. The resultant polymer mixture was precipitated in methanol, and the free polymer grown from the unfixed initiator was separated by 2 cycles of dissolving in benzene and centrifugation.

2.5. Surface-initiated polymerization using initiator-modified fumed silica in the absence of an unfixed initiator

30 ml of DMAc was added to 0.50–1.7 g of the initiator-modified fumed silica and 14.3 mg of CuBr (100 μmol) in a vacuum. After sonication of the mixture, 31.2 mg of bpy (200 μmol) in 30 ml of BMA was added, and the dispersion was kept at 60 °C for 2.5–9 h. The resultant poly(butyl methacrylate) (PBMA) grafted on the fumed silica was precipitated in methanol and dried under vacuum.

2.6. Blending with poly(vinyl chloride) (PVC)

Polymer blend films were obtained by casting from 5% solutions for mixtures of the PBMA samples and PVC ($M_n = 70$ k, Wako Pure Chemical) in tetrahydrofuran (THF). The films were dried and annealed at 110 °C for 6 h under vacuum.

2.7. Measurements

Thermogravimetry (TG): About 10 mg of the sample taken in a platinum pan was heated with a thermobalance (Rigaku, Thermo Plus TG 8120) from room temperature to 800 °C at a rate of 10 °C/min under an air flow (200 ml/min).

Differential scanning calorimetry (DSC): DSC measurements were performed with a differential scanning calorimeter (Q1000, TA Instruments) under an N_2 flow. About 5 mg of the sample was heated to 110 °C at a rate of 10 °C/min and then cooled to −20 °C at a rate of −10 °C/min. The sample was reheated to 110 °C at a rate of 10 °C/min. The second heating was used for characterization.

Size exclusion chromatography (SEC): SEC measurements were carried out at 30 °C using a system equipped with a refractive index detector (GPC-101, Shodex), and a set of three separation columns of 300 mm × 7.8 mm i.d. (TSKgel $G4000_{HR}$, Tosoh). THF was used as the eluent at a flow rate of 1.0 ml/min. The SEC system was calibrated with standard poly(methyl methacrylate) (PMMA) samples (M-75, Shodex). The PMMA calibration curve was modified for PBMA by universal calibration principle, where the Mark–Houwink parameters in THF were used; PMMA: $K = 9.55 \times 10^{-5}$ dL/g, $a = 0.719$, PBMA: $K = 1.48 \times 10^{-4}$ dL/g, $a = 0.664$ [39].

Scanning electron microscopy (SEM): The PBMA/silica composite sample was molded into a sheet by compression of 10 MPa at 90 °C. The surface of this thin sample which had been etched by an argon ion beam, was observed on a scanning electron microscope (S-5500, Hitachi) operated at an accelerating voltage of 2 kV.

Dynamic mechanical analysis (DMA): The annealed film samples were cut into rectangular specimens of 25 mm × 5 mm with ca. 0.12 mm thickness. Dynamic viscoelastic behaviors of the specimens were obtained using a dynamic mechanical analyzer (DVA-220, IT Keisokuseigyo) at a heating rate of 4 °C/min and a frequency of 1 Hz.

3. Results and discussion

3.1. Synthesis of the ATRP initiator with benzyl bromide moiety for immobilization

Benzyl bromide compounds react under moderate conditions with nucleophilic functional groups such as amino, carboxyl, phenolic hydroxyl, and mercapto groups. Therefore, benzyl bromide compounds having ATRP initiator moieties are useful for immobilization of the initiators on thus functionalized materials. For example, silica materials are easily modified with amines and thiols using the corresponding silane coupling agents. On the other hand, alkyl esters of 2-bromoisobutylic acid are suitable for the ATRP initiator because of the high initiation efficiency for many ATRP monomers [40]. Considering these facts, we have newly designed an ATRP initiator with a benzyl bromide moiety; *p*-(bromomethyl)benzyl 2-bromoisobutylate (BBnBiB). The BBnBiB was synthesized as Scheme 1.

The reactivity of the two alkyl bromide moieties in the BBnBiB compound, or the benzyl bromide and the 2-bromoisobutylate moieties, was checked out for amines; e.g., hexylamine, aniline, and *N*-butylaniline. The benzyl bromide moiety reacted with the aliphatic and aromatic amines even at room temperature [41], whereas the 2-bromoisobutylate moiety was inactive for these amines below 50 °C. However, the aliphatic amines seemed to abstract hydrogen bromide from the 2-bromoisobutylate moiety above 60 °C.

3.2. Synthesis of nanocomposites consisting of PBMA densely grafted on fumed silica

ATRP initiator-modified silica was synthesized as Scheme 2. Fumed silica which was composed of shapeless secondary particles formed by primary particles with a diameter of 14 nm, was treated

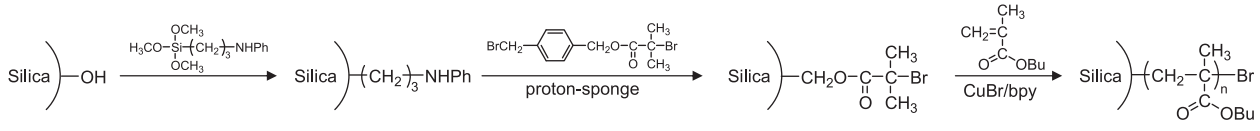

Scheme 2.

Table 2
Characteristics of the PBMA Samples for Blending with PVC.

Sample	$M_n \times 10^{-3}$	M_w/M_n	Fraction of fumed silica	
			Weight	Volume[b]
PBMA 120 k	118	1.15	–	–
Silica-PBMA 57 k	57[a]	–	0.25	0.14
Silica-PBMA 120 k	116[a]	–	0.14	0.077
Silica-PBMA 270 k	267[a]	–	0.069	0.036

[a] Estimated using the loading amount of the polymer chains on the fumed silica described in Table 1.
[b] Calculated using the bulk densities of 2.2 and 1.1 g/cm^3 for the fumed silica and the rest of organic phase containing PBMA, respectively.

with *N*-[3-(trimethoxysilyl)propyl]aniline (NHPh). This NHPh-modified fumed silica (Silica-NHPh) exhibited good dispersibility in AN in spite of its large specific surface area, and was successfully modified with BBnBiB in the presence of 1,8-bis(dimethylamino)-naphthalene (proton-sponge). In the reaction, hydrogen bromide generates as a byproduct, and the hydrogen bromide should be trapped by a base for quantitative conversion of the amine. The proton-sponge is suitable for the base because it is inactive for alkyl bromides including benzyl bromides in spite of a strong basicity. BMA was polymerized using this ATRP initiator-modified fumed silica, where an unfixed initiator, or benzyl 2-bromoisobutylate (BnBiB) was added in order to obtain a free polymer grown from the unfixed initiator for characterization. Several groups have reported that the average number molecular weights (M_n) of graft polymers were almost the same as the free polymers simultaneously formed in solution [19,21,24]. Fig. 1 shows TG curves of the modified fumed silica particles in an air flow. The loading amounts for the initiator-modified fumed silica (Silica-Br) and the PBMA-grafted fumed silica (Silica-PBMA), calculated from the weight losses from 180 to 800 °C in Fig. 1, are listed in Table 1 together with the SEC result for the corresponding free PBMA polymer. In the polymerization, the molecular weight distribution (M_w/M_n) of the free polymer is 1.10, indicating that the polymerization was sufficiently controlled. On the other hand, the graft density for Silica-PBMA cannot be calculated because the surface area of the fumed silica is not identified. Therefore, the graft density of PBMA in our method was tentatively determined using the same ATRP initiator fixed on a spherical silica with an average diameter of 500 nm (Supplementary data). Suppose that the graft density of the PBMA on the fumed silica is essentially the same as that on the 500 nm-spherical silica (0.54 chains/nm^2, Table S2), the graft surface area of the fumed silica is, in turn, estimated to be 56 m^2/g. This value of the 'effective' specific surface area is equivalent to that for a spherical silica with a diameter of 54 nm.

Surface-initiated polymerizations of BMA in the absence of the unfixed initiator, were also carried out using Silica-Br for preparation

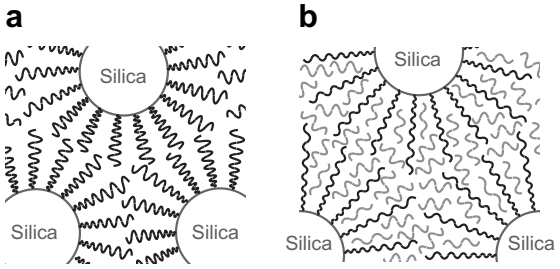

Fig. 3. Schematic drawings for the morphologies of (a) Silica-PBMA nanocomposite and (b) Silica-PBMA/PVC blend. The PBMA and PVC chains are respectively depicted in black and gray.

of blends with poly(vinyl chloride) (PVC). Three Silica-PBMA composites thus synthesized are summarized in Table 2. The M_ns of the graft polymers were estimated using the loading amount for the fumed silica shown in Table 1. The morphology of Silica-PBMA 270 k in condensed state, was observed by SEM, where the surface of the sample had been slightly etched by an argon ion beam in order that the PBMA polymer chains on the surface were removed out. Fig. 2 shows the SEM images of Silica-PBMA 270 k obtained at two magnifications. The SEM image at the low magnification in Fig. 2a suggests that fumed silica particles appeared to be homogeneously dispersed in the PBMA matrix. Each the particle clearly observed at the high magnification in Fig. 2b, must be an individual secondary particle formed by primary particles. The size of the secondary particle, 40–90 nm, is consistent with the ideal diameter calculated from the effective specific surface of the fumed silica.

3.3. Preparation of the densely grafted PBMA/PVC blends

In the case of polymer chains densely grafted on a nano-particle, the number of the polymer chains per unit area (hereafter referred to as chain density) is decreased as the chains are far from the curved surface of the particle, as shown in Fig. 3a. Therefore, it is expected that if a miscible different polymer is blended into the polymer brush, the miscible polymer chains are gradually enriched with increasing in the distance from the surface of the nano-particle (Fig. 3b). Here, we apply this strategy to the nanocomposites consisting of the PBMA densely grafted on the fumed silica.

In this study, PVC was used as a free polymer miscible with the graft PBMA, and the resultant blends were compared to conventional miscible blends of PBMA and PVC through DSC and DMA measurements. PBMA 120 k/PVC blends contained PVC weight fractions of 0.1, 0.3, 0.5, 0.7, and 0.9. Silica-PBMA/PVC blends were

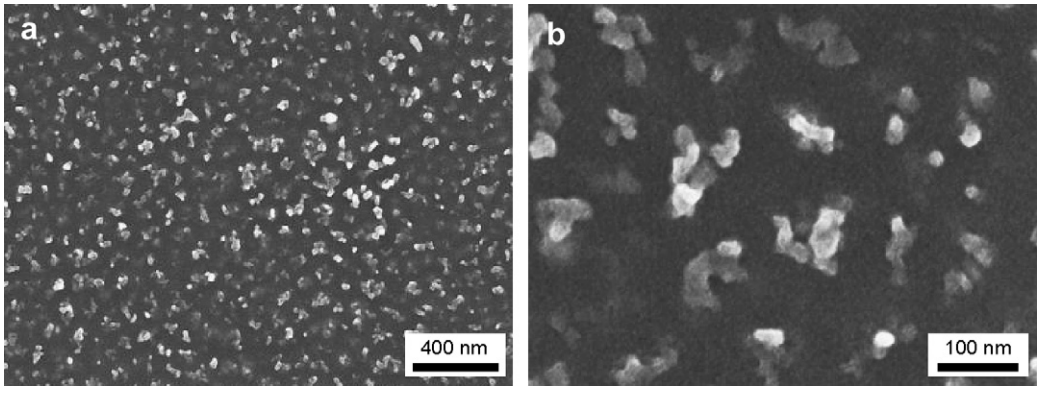

Fig. 2. SEM images of Silica-PBMA 270 k at (a) low and (b) high magnifications after argon etching.

designed to have the same PBMA/PVC weight ratios (r_{PBMA}) as PBMA 120 k/PVC blends; the added amounts of PVC were calculated on the basis of the net polymer contents in Silica-PBMA composites. All of the blends obtained by solution casting from THF, were annealed at 110 °C for 6 h under vacuum to attain to thermodynamically stable state.

3.4. Evaluation of the miscibility by DSC measurements

The miscibility of Silica-PBMA composites with PVC was evaluated by DSC. Fig. 4 shows derivative DSC (DDSC) curves of PBMA 120 k/PVC and Silica-PBMA 120 k/PVC. DDSC peaks are located around 35 °C and 84 °C respectively for PBMA 120 k and Silica-PBMA 120 k (Fig. 4a and b $r_{PBMA} = 10/0$), and PVC (Fig. 4a and b $r_{PBMA} = 0/10$). In addition, single DDSC peaks are observed for the both blend sample series in the temperature range from 43 °C to 83 °C depending on the weight ratio of PVC. However, the DDSC peaks for Silica-PBMA 120 k/PVC blends ($r_{PBMA} = 5/5$, and 3/7) are broadened to significantly differ from those for the corresponding PBMA/PVC blends. Notice that grafting of PBMA on the fumed silica have little impact on the DDSC trace (compare the DDSC curves at $r_{PBMA} = 10/0$ in Fig. 4a and b). This interesting finding is clearly explained by a wide gradient of the PVC concentration on a microscopic scale as shown in Fig. 3b; in Silica-PBMA 120 k/PVC blends, the PBMA component is enriched near the surface of the fumed silica, while the PVC component is enriched far from the surface. By contrast, at $r_{PBMA} = 1/9$, the DDSC peak for Silica-PBMA 120 k/PVC is sharper than that for the corresponding PBMA/PVC, showing a similar shape to that of the neat PVC. This is because excess PVC chains are excluded from the PBMA/PVC phase and localized around the mixed phase in Silica-PBMA 120 k/PVC. The localization of PVC is clearly confirmed from Fig. 5, where the peak-top temperatures of the DDSC traces in Fig. 4 are plotted as a function of the volume fraction of PVC. The peak-top temperatures for Silica-PBMA 120 k/PVC blends ($r_{PBMA} = 3/7$, and 1/9) are almost the same as that of PVC. Moreover, the peak-top temperatures for Silica-PBMA 120 k/PVC blends ($r_{PBMA} = 9/1$, 7/3, and 5/5) are also higher than those for the corresponding PBMA 120 k/PVC blends, which indicates formation of the PVC rich phase in Silica-PBMA 120 k/PVC blends.

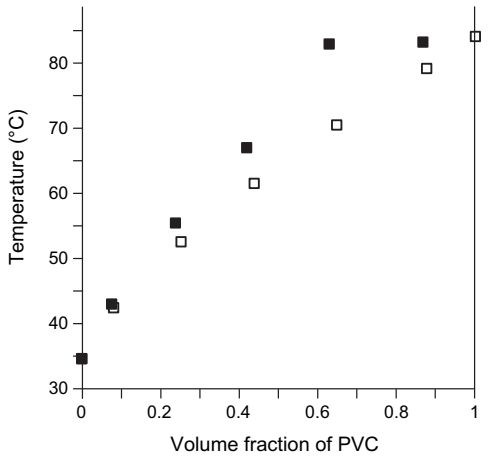

Fig. 5. Peak-top temperatures of the DDSC curves as a function of the volume fraction of PVC. (□) PBMA 120 k/PVC. (■) Silica-PBMA 120 k/PVC.

The effect of the chain density of the graft PBMA on the miscibility of Silica-PBMA/PVC blends was also examined by varying the M_n of the graft PBMA; lower M_n of the graft chains gives a higher average of the chain density in total, whereas higher M_n of the graft chains gives a lower average of the chain density. Fig. 6 shows DDSC curves of Silica-PBMA/PVC blends ($r_{PBMA} = 3/7$). There is a significant variation in the DDSC peaks depending on the M_n of the graft PBMA, or the average chain density. Considering that the DDSC peak of the neat PVC is observed 84 °C in Fig. 4, we can easily find

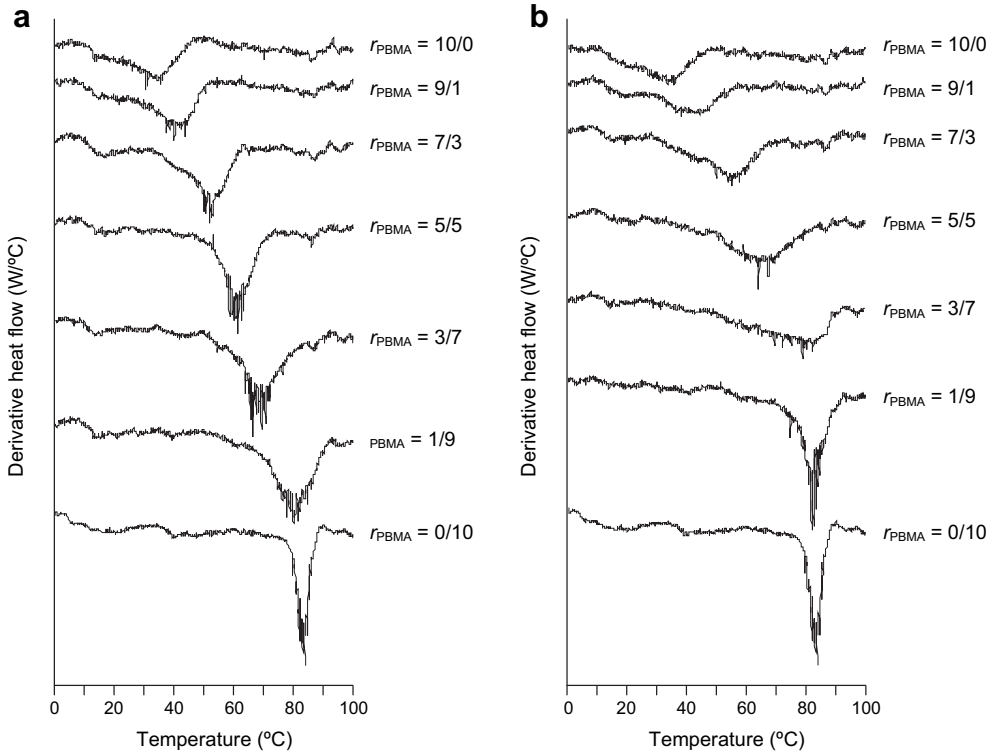

Fig. 4. Derivative DSC curves of (a) PBMA 120 k/PVC and (b) Silica-PBMA 120 k/PVC. The values of r_{PBMA} represent the weight ratios of PBMA/PVC.

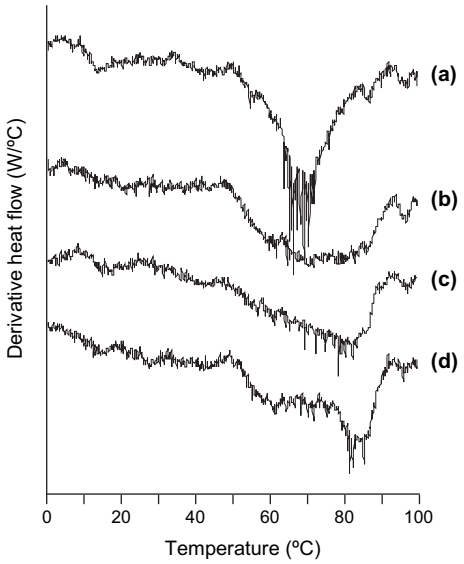

Fig. 6. Derivative DSC curves of the blends ($r_{PBMA} = 3/7$). (a) PBMA 120 k/PVC. (b) Silica-PBMA 270 k/PVC. (c) Silica-PBMA 120 k/PVC. (d) Silica-PBMA 57 k/PVC.

that the amount of a localized PVC is increased as the average chain density of the graft PBMA is increased. The localization of the PVC phase can be clearly seen for Silica-PBMA 57 k/PVC ($r_{PBMA} = 3/7$).

3.5. Dynamic viscoelastic behavior of the densely grafted PBMA/PVC blends

A fundamental mechanical property, or dynamic viscoelastic behavior was investigated for Silica-PBMA/PVC blends. Fig. 7 shows storage modulus (E′) and loss tangent (tanδ) curves of PBMA 120 k/PVC ($r_{PBMA} = 5/5$), Silica-PBMA 120 k/PVC ($r_{PBMA} = 5/5$), and PVC as a function of temperature. The storage modulus of Silica-PBMA 120 k/PVC is much higher than that of PBMA 120 k/PVC at the temperature less than 40 °C. However, the softening temperature of Silica-PBMA 120 k/PVC is slightly lower than that of PBMA 120 k/PVC, where the softening temperature is defined as a temperature at which storage modulus is suddenly decreased. On the other hand, the primary dispersion peak of Silica-PBMA 120 k/PVC is broader than that of PBMA 120 k/PVC, and the peak top temperature for Silica-PBMA 120 k/PVC is higher than that for PBMA 120 k/PVC by about 5 °C, which are consistent with the DSC results. Fig. 8 shows softening temperatures of PBMA 120 k/PVC and Silica-PBMA 120 k/PVC blends as a function of the volume fraction of PVC. Because softening temperatures are closely associated with glass-transition ones, the softening temperature of PBMA 120 k/PVC is increased as the weight ratio of PVC is increased. In the volume fraction of PVC more than 0.4, however, Silica-PBMA 120 k/PVC exhibits an almost constant value, which is much lower than those for PBMA 120 k/PVC. The lower softening temperature results from the PBMA rich phase near the fumed silica particle, where the mixed PVC amount is spatially restricted by the densely grafted PBMA chains, or the Silica-PBMA/PVC blend system has the upper limit of the softening temperature. This behavior strongly supports the gradient miscible state in the Silica-PBMA/PVC blend.

A synergistic effect was found on the storage modulus of Silica-PBMA/PVC blends. Fig. 9 shows storage moduluses of all of the blends at 20 °C, which is lower than the softening temperature of PBMA. The storage modulus for PBMA 120 k/PVC blends increases corresponding to the volume fraction of PVC, and the values are close to theoretical ones drawn by a broken line, which is straight line passing through the two extreme points of storage modulus. This is a typical behavior for miscible polymer blend systems. For Silica-PBMA 120 k/PVC, however, there are more increments in the storage modulus than are theoretically estimated (drawn by a solid line), especially at $r_{PBMA} = 7/3$ and 5/5. It is well-known for polymer blend systems that unlike mechanical strengths such as impact and tensile strengths, modulus is seldom subjected to synergistic effects. Nevertheless, the storage modulus of Silica-PBMA 120 k/PVC ($r_{PBMA} = 5/5$) are 32% higher than theoretical one in this system. In addition, the storage moduluses of Silica-PBMA 270 k/PVC and Silica-PBMA 57 k/PVC blends ($r_{PBMA} = 5/5$) are respectively 18% and 40% higher than corresponding theoretical ones (not drawn in Fig. 9), which indicates that this synergistic effect is closely related to the chain density of the graft PBMA. We consider that the synergistic effect on the storage modulus occurs as a result of two dominant factors; the densely grafted PBMA chains which radially spread over the matrix phase, and the gradient of the PVC concentration on a microscopic scale. It has been reported that even a concentrated polymer brush is further stretched in good solvent [42]. Also, in the case of Silica-PBMA/PVC blends, the densely grafted PBMA chains would be highly stretched due to the penetration of PVC. It would be possible that the highly stretched PBMA chains

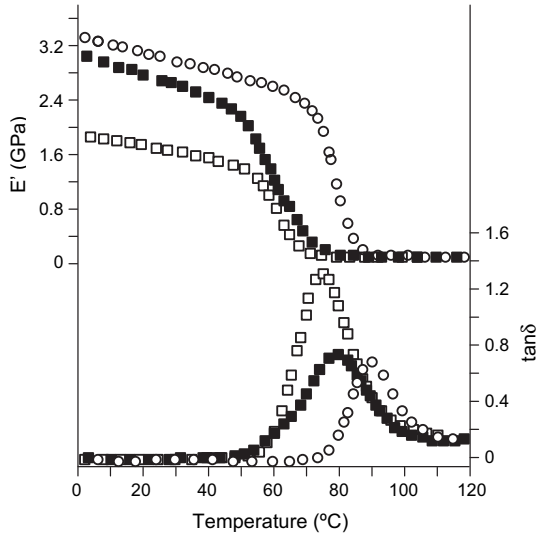

Fig. 7. Temperature-dependence of dymamic viscoelastic behaviors. (○) PVC. (□) PBMA 120 k/PVC ($r_{PBMA} = 5/5$). (■) Silica-PBMA 120 k/PVC ($r_{PBMA} = 5/5$).

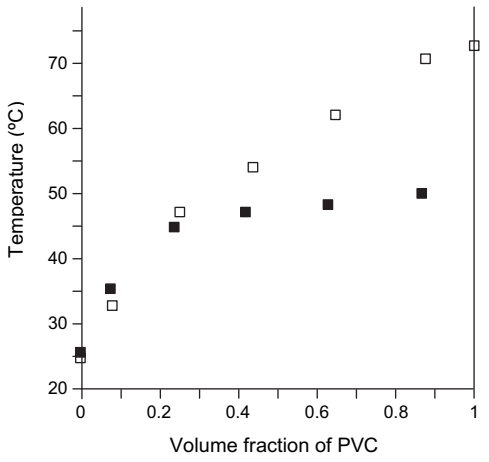

Fig. 8. Softening temperatures as a function of the volume fraction of PVC. (□) PBMA 120 k/PVC. (■) Silica-PBMA 120 k/PVC.

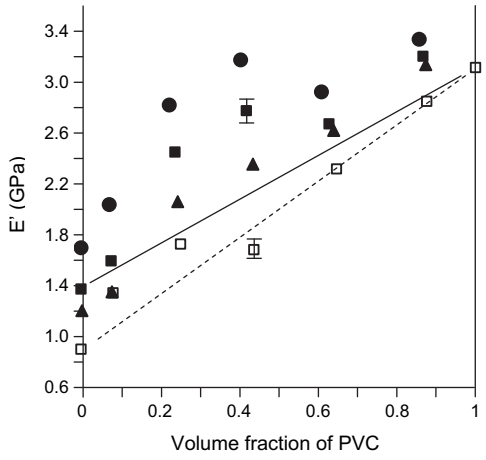

Fig. 9. Storage modulus as a function of the volume fraction of PVC at 20 °C. (□) PBMA 120 k/PVC. (▲) Silica-PBMA 270 k/PVC. (■) Silica-PBMA 120 k/PVC. (●) Silica-PBMA 57 k/PVC. Theoretical storage modulus curves for PBMA 120 k/PVC and Silica-PBMA 120 k/PVC blends are respectively drawn by broken and solid lines.

behave like a stiff filler. Secondly, this blend system is further reinforced with a PVC rich phase produced by the gradient of the PVC concentration. The PVC rich phase makes possible the formation of a stiff matrix phase in Silica-PBMA/PVC blends; PVC has higher storage modulus than PBMA. The PVC content is also important. In Fig. 9, drops in the storage modulus at $r_{PBMA} = 3/7$ for Silica-PBMA 57 k/PVC and Silica-PBMA 120 k/PVC are observed, suggesting that too much PVC content spoils in the synergistic effect for the blend system, where the somewhat localizations of the PVC are confirmed as shown in Fig. 6c,d.

This type of miscible blend system provides a new concept of polymer materials. In the new blend system, the high chain density of the graft polymer is important according to the chain density dependence of the storage modulus exhibited in Fig. 9. The densely grafted polymer gives this blend system the continuously varied phase with the wide blend gradient. The blend system in this study, therefore, should also demonstrate its potential abilities for tensile and impact strengths, because these mechanical properties more affected than the storage modulus by the heterogeneous morphology mentioned above. In this sense, the new blend system is similar to block copolymer systems and mixed polymer systems adopting sea-island structures. However, our blend system has the further advantage of strengthening by the graft polymer chains over such materials. Further studies on the new blend system for the mechanical properties are currently in progress.

In conclusion, we have synthesized PBMA/fumed silica composites by surface-initiated ATRP. In these syntheses, a newly designed initiator, *p*-(bromomethyl)benzyl 2-bromoisobutylate made possible the immobilization of the initiator on the fumed silica. The PBMA densely grafted on the fumed silica has exhibited unusual miscibility with PVC through DSC and DMA measurements. This interesting finding is due to a wide gradient of the PVC concentration on a microscopic scale, resulting from the graft PBMA chains. Furthermore, a synergistic effect on storage modulus was seen in the densely grafted PBMA/PVC blends. A possible explanation is suggested that the PBMA chains highly stretched owing to penetration of PVC behaved like a stiff filler.

Acknowledgements

SEM observations were carried out by Mr. Hiroaki Kadoura and Ms. Yoriko Matsuoka at Toyota Central R&D Labs., Inc., and the authors deeply appreciate their help.

Appendix. Supplementary data

The Supplementary material associated with this article can be found at doi:10.1016/j.polymer.2009.11.008.

References

[1] Usuki A, Kojima Y, Kawasumi M, Okada A, Kurauchi T, Kamigaito O. J Mater Res 1993;8:1174.
[2] Usuki A, Kojima Y, Kawasumi M, Okada A, Kurauchi T, Kamigaito O. J Mater Res 1993;8:1179.
[3] Kato M, Usuki A, Okada A. J Appl Polym Sci 1997;66:1781.
[4] Kawasumi M, Hasegawa N, Kato M, Usuki A, Okada A. Macromolecules 1997;30:6333.
[5] Barnes KA, Karim A, Douglas JF, Nakatani AI, Gruell H, Amis EJ. Macromolecules 2000;33:4177.
[6] Lee JY, Thompson R, Jasnow D, Balazs AC. Phys Rev Lett 2002;89:155503.
[7] Liu J, Tanaka T, Sivula K, Alivisatos AP, Frechet MJ. J Am Chem Soc 2004; 126:6550.
[8] Mackay ME, Tuteja A, Duxbury PM, Hawker CJ, Horn BV, Guan Z, et al. Science 2006;311:1740.
[9] Balazs AC, Emrick T, Russell TP. Science 2006;314:1107.
[10] Radhakrishnan B, Ranjan R, Brittain WJ. Soft Matter 2006;2:386.
[11] Zou H, Wu S, Shen J. Chem Rev 2008;108:3893.
[12] Krenkler KP, Laible R, Hamann K. Angew Makromol Chem 1978;53:101.
[13] Bridger K, Vincent B. Eur Polym J 1980;16:1017.
[14] Tsubokawa N, Hosoya M, Yanadori K, Sone YJ. Macromol Sci Chem 1990; A27:445.
[15] Hamann R, Laible R. Angew Makromol Chem 1973;48:97.
[16] Boven G, Oosterling MLCM, Challa G, Schouten AJ. Polymer 1990;31:2377.
[17] Tsubokawa N, Kougur S, Maruyama K, Sone Y, Shimomura M. Polym J 1990; 22:827.
[18] Pattern TE, Matyjaszewski K. Adv Mater 1998;10:1.
[19] von Werne T, Pattern TE. J Am Chem Soc 2001;123:7497.
[20] Marutani E, Yamamoto S, Ninjbadgar T, Tsujii Y, Fukuda T, Takano M. Polymer 2004;45:2231.
[21] El Harrak A, Carrot G, Oberdisse J, Eychenne-Baron C, Boue F. Macromolecules 2004;37:6376.
[22] El Harrak A, Carrot G, Oberdisse J, Jestin J, Boué F. Polymer 2005;46:1095.
[23] Wang Y-P, Pei X-W, He X-Y, Lei Z-Q. Eur Polym J 2005;41:737.
[24] Ohno K, Morinaga T, Koh K, Tsujii Y, Fukuda T. Macromolecules 2005;38:2137.
[25] Yang Q, Wang L, Xiang W, Zhou J, Tan Q. Polymer 2007;48:3444.
[26] Czaun M, Mizanur Rahman M, Takafuji M, Ihara H. Polymer 2008;49:5410.
[27] Chen R, Maclaughlin S, Botton G, Zhu S. Polymer 2009;50:4293.
[28] Wang JS, Matyjaszewski K. J Am Chem Soc 1995;117:5614.
[29] Kato M, Kamigaito M, Sawamoto M, Higashimura T. Macromolecules 1995; 28:1721.
[30] Chiefari J, Chong YK, Ercole F, Krstina J, Jeffery J, Le TPT, et al. Macromolecules 1998;31:5559.
[31] Yamamoto S, Tsujii Y, Fukuda T. Macromolecules 2002;35:6077.
[32] Urayama K, Yamamoto S, Tsujii Y, Fukuda T, Neher D. Macromolecules 2002;35:9459.
[33] Tsujii Y, Ohno K, Yamamoto S, Goto A, Fukuda T. Adv Polym Sci 2006;197:1.
[34] Ohno K, Morinaga T, Takeno S, Tsujii Y, Fukuda T. Macromolecules 2006; 39:1245.
[35] Kern RJ. J Polym Sci 1958;33:524.
[36] Walsh DJ, McKeown JG, Kern RJ. Polymer 1980;21:1330.
[37] Perrin P, Prud'homme RE. Polymer 1991;32:1468.
[38] Breschi MC, Calderone V, Digiacomo M, Macchia M, Martelli A, Martionotti E, et al. J Med Chem 2006;49:2628.
[39] Pusch J, van Herk AM. Macromolecules 2005;38:6939.
[40] Tang W, Matyjaszewski K. Macromolecules 1858;2007:40.
[41] Radhakrishnamurti PS, Panigrahi GP. Bull Chem Soc Jpn 1970;43:81.
[42] Yamamoto S, Ejaz M, Tsujii Y, Matsumoto M, Fukuda T. Macromolecules 2000;33:5602.